

Soliton structures in the (1+1)-dimensional Ginzburg-Landau equation with a parity-time-symmetric potential in ultrafast optics

Wenyi Li(李文义), Guoli Ma(马国利), Weitian Yu(于维天), Yujia Zhang(张玉佳), Mengli Liu(刘孟丽), Chunyu Yang(杨春玉), Wenjun Liu(刘文军)
Citation: Chin. Phys. B . 2018, 27(3): 030504. **doi:** 10.1088/1674-1056/27/3/030504

Journal homepage: http://cpb.iphy.ac.cn; http://iopscience.iop.org/cpb

What follows is a list of articles you may be interested in

Periodic solitons in dispersion decreasingfibers with a cosine profile

Jia Ren-Xu, Yan Hong-Li, Liu Wen-Jun, Lei Ming
Chin. Phys. B . 2014, 23(10): 100502. **doi:** 10.1088/1674-1056/23/10/100502

Interactions among special embed-solitons for the (3+1)-dimensional Burgers equation

Zhang Wen-Ting, Dai Chao-Qing, Chen Wei-Lu
Chin. Phys. B . 2013, 22(4): 040509. **doi:** 10.1088/1674-1056/22/4/040509

Propagation of electromagnetic soliton in anisotropic biquadratic ferromagnetic medium

L. Kavitha, M. Saravanan, D. Gopi
Chin. Phys. B . 2013, 22(3): 030512. **doi:** 10.1088/1674-1056/22/3/030512

Non-completely elastic interactions in (2+1)-dimensional dispersive long wave equation

Chen Wei-Lu, Zhang Wen-Ting, Zhang Li-Pu, Dai Chao-Qing
Chin. Phys. B . 2012, 21(11): 110507. **doi:** 10.1088/1674-1056/21/11/110507

Feshbach resonance management of vector solitons in two-component Bose–Einstein condensates

Wang Qiang, Wen Lin, Li Zai-Dong
Chin. Phys. B . 2012, 21(8): 080501. **doi:** 10.1088/1674-1056/21/8/080501

Soliton structures in the (1+1)-dimensional Ginzburg–Landau equation with a parity-time-symmetric potential in ultrafast optics*

Wenyi Li(李文义)[1,2], Guoli Ma(马国利)[1,2], Weitian Yu(于维天)[1], Yujia Zhang(张玉佳)[1], Mengli Liu(刘孟丽)[1,2], Chunyu Yang(杨春玉)[1], and Wenjun Liu(刘文军)[1,2,†]

[1] *State Key Laboratory of Information Photonics and Optical Communications, School of Science, Beijing University of Posts and Telecommunications, Beijing* 100876, *China*

[2] *Beijing National Laboratory for Condensed Matter Physics, Institute of Physics, Chinese Academy of Sciences, Beijing* 100190, *China*

(Received 30 September 2017; revised manuscript received 10 November 2017; published online 10 February 2018)

In this paper, the (1+1)-dimensional variable-coefficient complex Ginzburg–Landau (CGL) equation with a parity-time (PT) symmetric potential $U(x)$ is investigated. Although the CGL equations with a PT-symmetric potential are less reported analytically, the analytic solutions for the CGL equation are obtained with the bilinear method in this paper. Via the derived solutions, some soliton structures are presented with corresponding parameters, and the influences of them are analyzed and studied. The single-soliton structure is numerically verified, and its stability is analyzed against additive and multiplicative noises. In particular, we study the soliton dynamics under the impact of the PT-symmetric potential. Results show that the PT-symmetric potential plays an important role for obtaining soliton structures in ultrafast optics, and we can design fiber lasers and all-optical switches depending on the different amplitudes of soliton-like structures.

Keywords: solitons, parity-time symmetry, Ginzburg–Landau equation, bilinear method

PACS: 05.45.Yv, 42.65.Tg **DOI:** 10.1088/1674-1056/27/3/030504

1. Introduction

The concept of the parity-time (PT) symmetry was put forward in the quantum mechanics firstly in 1998.[1] Since then, the research of the PT symmetry has attracted much attention. The first relation between the PT symmetry and optics field has been found by Musslimani,[2] and the first theoretical relation of PT-symmetric matter waves in the Bose–Einstein condensates with the harmonic potential had been found by Yan *et al.*[3–5] The realization of the PT symmetry in the optical materials had been achieved in 2009.[6] A more impressive extension as the pseudo-PT symmetry has been proposed.[7]

In quantum theory, if a general Hamiltonian $\hat{H} = (\hat{p}^2/2) + \hat{V}(x)$ (p and x respectively signify momentum and position operator) is PT-symmetric, it should obey the necessary condition that (not sufficient) $V(x) = V^*(x)$ (* stands for the complex conjugation).[2] In optics, the potential $V(x)$ plays as an optical potential by a complex refractive-index distribution $n(x) = n_{\mathrm{R}}(x) + \mathrm{i}n_{\mathrm{I}}(x)$, wherein the real component and the imaginary part denote respectively the refractive index profile and the gain (+) or loss (-) in the system. The PT-symmetric conditions mean $n_{\mathrm{R}}(x) = n_{\mathrm{R}}(-x)$ and $n_{\mathrm{I}}(x) = -n_{\mathrm{I}}(-x)$, that is to say, the index distribution must be an even function of position, whereas the gain or loss must be an odd function.[8–13] In addition, the spectrums of the PT-symmetry system would appear to be complex while changing some appropriate parameters,[14–19] which can be used to realize the PT symmetry coupler.[20] Recently, symmetry breaking of solitons in special types of PT-symmetric potentials had been reported regardless of PT symmetry breaking or not.[21–23]

For the realistic optical systems, the optical lattices (OLs) and waveguides with the PT-symmetry have been studied for many different cases. The gap soliton had been found in the linear OLs, and the influence of competing nonlinearities had been analyzed.[24–26] To the nonlinear OLs, the multipole solitons, multistable solitons and matter-wave solitons had been revealed.[27–29] With regard to the optical waveguides, the rich dynamics and stability of solitons in different structures as dual-core, double-channel and arrays has been studied.[30–32] The dynamics of solitons are described by the nonlinear Schrödinger equation (NLS),[33–40] and can be used in mode-locked fiber lasers.[41–44] Moreover, compared to those mentioned above, the research of the PT-symmetric laser system is rarely reported. The pulse evolution can be described by the complex Ginzburg–Landau (CGL) equation in the laser cavities.[45–48] With the triangle PT-symmetric potential, soliton drift and decay stemmed from the linear loss modulation.[49] Some applications as realizing the single mode transmission in the semiconductor laser have been reported recently.[50,51]

Compared with the constant coefficient CGL equation, those variable-coefficient CGL equations are able to de-

*Project supported by the National Natural Science Foundation of China (Grant No. 11674036), the Beijing Youth Top-notch Talent Support Program, China (Grant No. 2017000026833ZK08), and the Fund of State Key Laboratory of Information Photonics and Optical Communications (Beijing University of Posts and Telecommunications) (Grant Nos. IPOC2016ZT04 and IPOC2017ZZ05).

†Corresponding author. E-mail: wjliu@iphy.ac.cn

© 2018 Chinese Physical Society and IOP Publishing Ltd

scribe multifarious situations more powerfully in such natural phenomena as the coastal waters of oceans, optical-fiber communications and blood vessels.[52–54] In variable-coefficient models, the general NLS equation and CGL equation have been widely investigated than that with PT-symmetric potentials;[55,56] especially, the variable-coefficient CGL equation with a PT-symmetric potential has been less reported but worthwhile to further research.[57,58]

In this paper, we will study the (1+1)-dimensional variable-coefficient CGL equation, which can be divided into two situations: when the variable coefficients are real, it can be described by the NLS equation. Nevertheless, when the variable coefficients are complex, it is the CGL equation. Here, we discuss the CGL equation with a PT-symmetric potential, and regard the NLS model as its special case. It will be organized as follows. In Section 2, we will describe the (1+1)-dimensional variable-coefficient CGL equation which includes two different circumstances, and the solution method will be constructed. In Section 3, we will illustrate and discuss different structures of the solutions received, and perform numerical simulation with noises. In Section 4, results will be summarized.

2. Model and solution

The (1+1)-dimensional variable-coefficient CGL equation with the harmonic for the dimensionless light field $u(z,x)$ has the form,[59]

$$\mathrm{i}u_z+\beta(x)u_{xx}+\gamma(x)|u|^2u+U(x)u=0, \tag{1}$$

where z is the dimensionless propagation distance, and the variable coefficients $\beta(x)$, $\gamma(x)$, and $U(x)$ are respectively the diffraction, nonlinearity, and harmonic potential coefficients. Using the separation of variables, we define the solution $u(z,x)$ as

$$u(z,x)=f(x)A(z,x). \tag{2}$$

Substituting Eq. (2) into Eq. (1), we obtain two equations as a result of the separation of variables. They are

$$\mathrm{i}A_z+2\beta(x)\frac{f_x}{f}A_x+\beta(x)A_{xx}+\gamma(x)|f|^2|A|^2A=0, \tag{3}$$

$$\frac{f_{xx}}{f}=-\frac{U(x)}{\beta(x)}. \tag{4}$$

Here, equation (3) can be abbreviated as

$$\mathrm{i}A_z+\alpha(x)A(x)+\beta(x)A_{xx}+\sigma(x)|A|^2A=0 \tag{5}$$

with

$$\alpha(x)=2\beta(x)\frac{f_x}{f},\sigma(x)=\gamma(x)|f|^2. \tag{6}$$

Firstly, we use the dependent variable transformation

$$A(z,x)=\frac{G(z,x)}{F(z,x)}, \tag{7}$$

where $G(z,x)$ and $F(z,x)$ are complex differentiable functions. Submitting expression (7) into Eq. (5), we can obtain the bilinear forms for Eq. (5) as

$$\mathrm{i}D_zG\cdot F+\alpha(x)D_xG\cdot F+\beta(x)D_x^2G\cdot F=0, \tag{8}$$

$$\beta(x)D_x^2F\cdot F-\sigma(x)|G|^2=0, \tag{9}$$

where D_z and D_x are the Hirota's bilinear operators,[60] which can be defined by

$$D_z^mD_x^n(a\cdot b)=\left(\frac{\partial}{\partial z}-\frac{\partial}{\partial z'}\right)^m\left(\frac{\partial}{\partial x}-\frac{\partial}{\partial x'}\right)^n a(z,x)b(z',x')|_{z'=z,x'=x}.$$

Here, the expressions of $G(z,x)$ and $F(z,x)$ are as follows:

$$\begin{aligned}&G(z,x)=\varepsilon G_1(z,x),\\&F(z,x)=1+\varepsilon^2F_2(z,x),\\&G_1=\mathrm{e}^{(k_1+\mathrm{i}k_2)+(w_1(x)+\mathrm{i}w_2(x))+(\theta_1+\mathrm{i}\theta_2)},\end{aligned} \tag{10}$$

where ε is a formal expansion parameter, k_1,k_2,θ_1, and θ_2 are real constants. $w_1(x)$ and $w_2(x)$ are the differentiable functions to be determined.

3. Analysis and discussion

This section can be divided into two cases with different conditions depending whether the coefficients are complex or not.

3.1. Coefficients are real

As a special example, equation (1) can be regarded as a NLS model. Firstly, we consider Eq. (5).[61] Substituting expressions (10) into bilinear forms (8) and (9), and equating coefficients of the same powers of ε to zero yield the following expressions of $F_2(x),\sigma(x),\alpha(x),\beta(x)$ about $w_1(x)$ and $w_2(x)$.

$$\begin{aligned}F_2(z,x)&=m(x)\,\mathrm{e}^{2k_1z+2w_1(x)+2\theta_1},\ m(x)=c_1\,\mathrm{e}^{c_2x-2w_1(x)},\\w_2(x)&=c_3x+c_6,\ \gamma(x)=\frac{\sigma(x)}{|f(x)|^2},\\\sigma(x)&=-((2k_1w_1'(x)+2k_2w_2'(x))(4m'(x)w_1'(x)+m''(x)\\&\quad+4m(x)w_1'(x)^2+2m(x)w_1''(x)))/(w_1'(x)^2w_2'(x)\\&\quad+w_2'(x)^3-w_2'(x)w_1''(x)+w_1'(x)w_2''(x)),\\\beta(x)&=(-k_1w_1'(x)-k_2w_2'(x))/(w_1'(x)^2w_2'(x)+w_2'(x)^3\\&\quad-w_2'(x)w_1''(x)+w_1'(x)w_2''(x)),\\\alpha(x)&=(k_1w_1'(x)^2+2k_2w_1'(x)w_2'(x)-k_1w_2'(x)^2+k_1w_1''(x)\\&\quad+k_2w_2''(x))/(w_1'(x)w_2'(x)+w_2'(x)^3-w_2'(x)w_1''(x)\\&\quad+w_1'(x)w_2''(x)),\\w_1(x)&=c_5+\frac{1}{2}\left(c_2x-2\log\left(\cos\left(\frac{1}{2}c_4(-c_2^2k_1^2-4c_3^2k_1\right.\right.\right.\end{aligned}$$

$$-4c_2c_3k_2)^{1/2}-\frac{\sqrt{-c_2^2k_1+4c_3^2k_1-4c_2c_3k_2x}}{2\sqrt{k_1}}\Bigg)\Bigg)\Bigg), \tag{11}$$

where c_i $(i=1,2,3,4,5,6)$ are real constants. Substituting Eqs. (10)–(11) into Eq. (7), we can get the expression of $A(z,x)$ as follows:

$$A(z,x) = \frac{\varepsilon\, \mathrm{e}^{\frac{c_2x}{2}+\mathrm{i}c_3x+c_5+\mathrm{i}c_6+k_1z+\mathrm{i}k_2z+\theta_1+\mathrm{i}\theta_2}}{1+c_1\,\mathrm{e}^{c_2x+2k_1z+2\theta_1}\varepsilon^2} \times \sec\left(\frac{\sqrt{-c_2^2k_1+4c_3^2k_1-4c_2c_3k_2}(c_4k_1-x)}{2\sqrt{k_1}}\right). \tag{12}$$

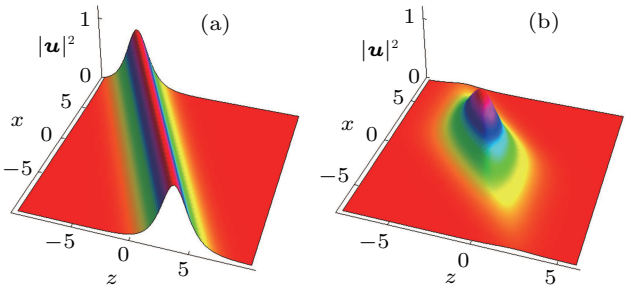


Fig. 1. (color online) Different soliton structures of $A(z,x)$ with the appropriate parameters: (a) Single soliton structure with $\varepsilon=1$, $k_1=1$, $k_2=0.75$, $c_1=2$, $c_i=1$ $(i=2,3,4,5,6)$ and $\theta_i=1$ $(i=1,2)$. (b) Dromion structure with $\varepsilon=1$, $k_i=1$ $(i=1,2)$, $c_i=1$ $(i=1,2,3,4,5,6)$ and $\theta_i=1$ $(i=1,2)$.

Then, combining Eq. (11) with Eqs. (4)–(6), we obtain

$$f(x) = c\,\mathrm{e}^{\int\frac{\alpha(x)}{2\beta(x)}\mathrm{d}x} = c\cos\left(\frac{\sqrt{-c_2^2k_1+4c_3^2k_1-4c_2c_3k_2}(c_4k_1-x)}{2\sqrt{k_1}}\right), \tag{13}$$

where c is a real constant similarly with c_i $(i=1,2,3,4,5,6)$. Specially, the value of $U(x)$ is always a constant, and

$$U(x)=\frac{-\alpha(x)^2-2\alpha'(x)\beta(x)+2\alpha(x)\beta'(x)}{4\beta(x)}=C. \tag{14}$$

Here, C is a constant, and it varies with different parameters. Substituting Eqs. (12)–(13) into Eq. (2), we acquire the following expression of $u(z,x)$:

$$u(z,x)=c\varepsilon\frac{\mathrm{e}^{\frac{c_2x}{2}+\mathrm{i}c_3x+c_5+\mathrm{i}c_6+k_1z+\mathrm{i}k_2z+\theta_1+\mathrm{i}\theta_2}}{1+c_1\,\mathrm{e}^{c_2x+2k_1z+2\theta_1}\varepsilon^2}. \tag{15}$$

From Figs. 2(a) and 3(b), we find that they have diverse amplitudes and pulse widths due to the different diffraction coefficient $\beta(x)$. With $\beta(x)$ enlarged, the amplitude becomes higher, and the pulse duration becomes narrower. That is to say, the energy of the soliton becomes bigger. In contrast to $\beta(x)$, from Figs. 3(a) and 3(b), we can find that the amplitude becomes lower, and the pulse duration becomes wider with the nonlinearity $\gamma(x)$ enlarged; in other words, the energy of the soliton becomes smaller. In addition, changing the signs of $\beta(x)$ and $\gamma(x)$ simultaneously, they can change the direction of the propagation. However, when they have the same sign, equation (1) does not have soliton solutions. Probably due to the constant coefficient bound potential modulation, it is only a single soliton structure of $u(z,x)$.

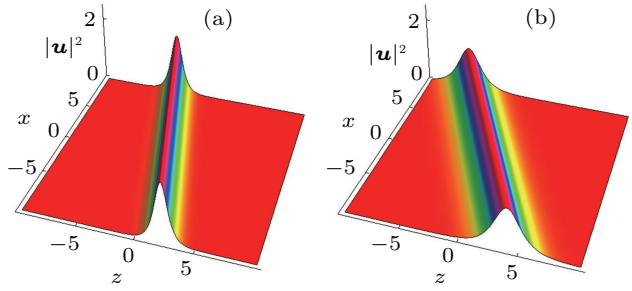


Fig. 2. (color online) Influence of the diffraction $\beta(x)$. Parameters are as follows: (a) $\beta(x)=2$, $\gamma(x)=-2/e^2$, $\varepsilon=1$, $k_1=2$, $k_2=1$, $c_1=0.5$, $c_i=1$ $(i=2,3,4,5,6)$ and $\theta_i=1$ $(i=1,2)$; (b) $\beta(x)=1$, $\gamma(x)=-2/e^2$, $\varepsilon=1$, $k_i=1$ $(i=1,2)$, $c_3=-1$, $c_i=1$ $(i=2,4,5,6)$, and $\theta_i=1$ $(i=1,2)$.

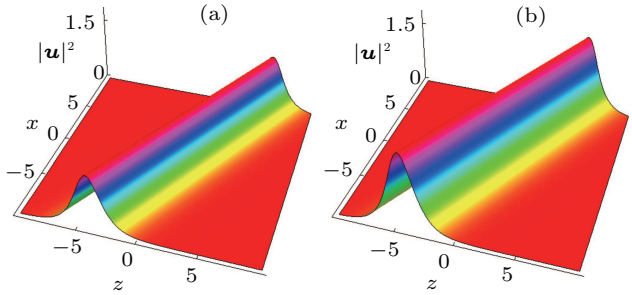


Fig. 3. (color online) Influence of the nonlinearity $\gamma(x)$. Parameters are as follows: (a) $\beta(x)=-1$, $\gamma(x)=2/e^2$, $\varepsilon=1$, $k_1=-1$, $k_2=1$, $c_3=-1$, $c_i=1$ $(i=2,4,5,6)$ and $\theta_i=1$ $(i=1,2)$; (b) $\beta(x)=-1$, $\gamma(x)=1/e^2$, $\varepsilon=1$, $k_1=-1$, $k_2=1$, $c_3=-1$, $c_i=1$ $(i=2,4,5,6)$ and $\theta_i=1$ $(i=1,2)$.

To verify the accuracy of the analytic solution, we use the split-step Fourier method[65] to simulate the beam propagation. As shown in Fig. 4, the initial beam keeps balance to propagate under the focusing and anomalous dispersion conditions.

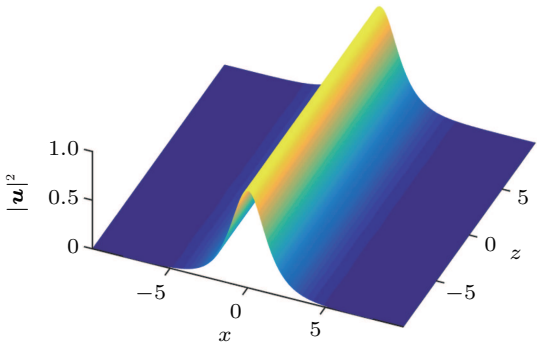


Fig. 4. (color online) Numerical simulation of solitons with the appropriate parameters as: $\alpha=0.5$, $\beta=-1$, and $\sigma=2$.

In order to study the stability of this structure, we consider the influences of additive and multiplicative noises.[64] Firstly, we discuss the structure against additive noises. We define that

the strength radio is noise variance compared to the input maximum amplitude. Here we set initial input sech(x), and we find that the soliton is stable against 10% additive noises with some compressions. When the strength radio increases to 50%, the soliton evolves into breather-like structure, and gradually disappears. Furthermore, the structure is completely destroyed under 100% noises. In order to improve the signal transmission quality, decreasing nonlinearity to 0.5 can recover the signal.

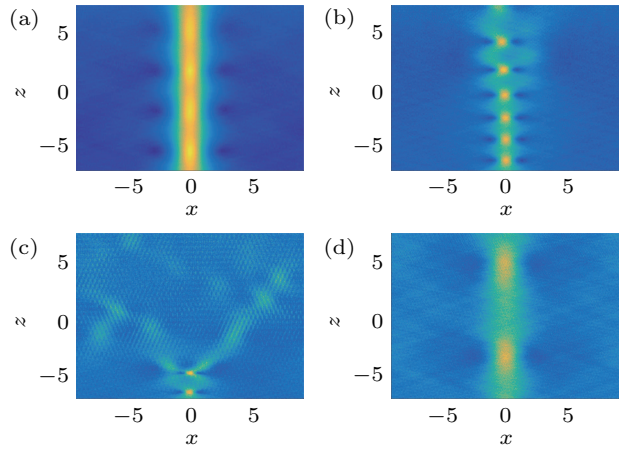


Fig. 5. (color online) With the same parameters as Fig. 4, the soliton simulation against additive noises with following strength radio: (a) 10%, (b) 50%, (c) 100%. (d) According to panel (c), we recover the signal setting $\sigma = 0.5$.

As the other aspect, the multiplicative noises have more disruptive to signals rather than the additive noises. The signal is completely distorted while the strength ratio of the multiplicative noise is just 0.1%. If we increase the nonlinearity to 9, we can obtain a rough channel to transfer the signal due to the focusing effect. In addition, decreasing the dispersive effect can further focus the signal, and form a breather-like structure.

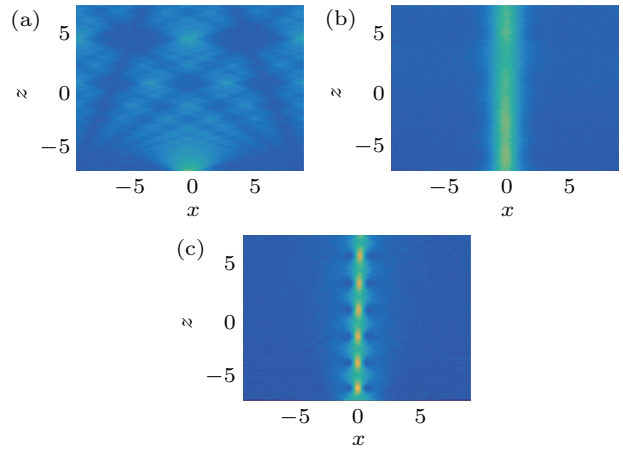


Fig. 6. (color online) With the same parameters as Fig. 4, the soliton simulation against multiplicative noises. (a) The strength radio is 10%. (b) We set $\sigma = 9$. (c) Based on (b), we set $\beta = -0.34$.

3.2. Coefficients are complex

Obviously, equation (5) is a GL model. We also consider Eq. (5) firstly. The solution is the same with Section 3.1, but in this part the complex coefficients should be taken into account. That is to say, the expressions of the complex coefficients are

$$\begin{aligned}\alpha(x) &= \alpha_1(x) + \mathrm{i}\alpha_2(x),\\ \sigma(x) &= \sigma_1(x) + \mathrm{i}\sigma_2(x),\\ \beta(x) &= \beta_1(x) + \mathrm{i}\beta_2(x),\end{aligned} \tag{16}$$

where $\alpha_i(x), \sigma_i(x)$, and $\beta_i(x)$ $(i = 1,2)$ are all real functions. By calculating the expressions of $\alpha_i(x), \sigma_i(x)$ $(i = 1,2)$, and $\beta_i(x)$ $(i = 1,2)$, we obtain

$$\begin{aligned}
F_2(z,x) &= m(x)\,\mathrm{e}^{2k_1 z + 2w_1(x) + 2\theta_1},\\
m(x) &= c_2\,\mathrm{e}^{c_1 x - 2w_1(x)},\\
\gamma(x) &= \frac{\sigma_1(x) + \sigma_2(x)}{|f(x)|^2},\\
\sigma_1(x) &= 2c_1^2 c_2\,\mathrm{e}^{c_1 x - 2w_1(x)}\beta_1(x),\\
\sigma_2(x) &= 2c_1^2 c_2\,\mathrm{e}^{c_1 x - 2w_1(x)}\beta_2(x),\\
\alpha_1(x) &= \frac{1}{w_1'(x)^2 + w_2'(x)^2}(-\beta_1(x)w_1'(x)^3\\
&\quad + \beta_2(x)w_1'(x)^2 w_2'(x) + w_2'(x)(-k_1 + \beta_2(x)w_2'(x)^2\\
&\quad - \beta_2(x)w_1''(x) - \beta_1(x)w_2''(x)) + w_1'(x)\\
&\quad \times (k_2 - \beta_1(x)w_2'(x)^2 + w_1''(x)\\
&\quad + \beta_2(x)w_2''(x))),\\
\alpha_2(x) &= -\frac{1}{w_1'(x)^2 + w_2'(x)^2}(\beta_2(x)w_1'(x)^3\\
&\quad + \beta_1(x)w_1'(x)^2 w_2'(x) + w_1'(x)(k_1 + \beta_2(x)w_2'(x)^2\\
&\quad + \beta_2(x)w_1''(x) + \beta_1(x)w_2''(x)) + w_2'(x)\\
&\quad \times (k_2 + \beta_1(x)w_2'(x)^2 - \beta_1(x)w_1''(x) + \beta_2(x)w_2''(x))),\\
\beta_1(x) &= (c_1 k_2 w_2'(x)^2 - 2k_1 w_2'(x)^3 - w_1'(x)^2\\
&\quad \times (c_1 k_2 + 2k_1 w_2'(x)) - k_1 w_2'(x)(c_1^2 + 2w_1''(x))\\
&\quad + c_1(k_2 w_{''}(x) - k_1 w_2''(x)) + w_1'(x)\\
&\quad \times (c_1^2 k_2 + 2c_1 k_1 w_2'(x) + 2k_1 w_2''(x)))\\
&\quad /(c_1(-2c_1 w_1'(x)^3 + w_1'(x)^4 + w_2' x^4)\\
&\quad + w_1'(x)^2(c_1^2 + 2w_2(x)^2 - 2w_1''(x)) + w_1''(x)^2\\
&\quad + w_2'(x)^2(c_1^2 + 2w_1''(x)) + 2c_1 w_2'(x)w_2''(x) + w_2''(x)\\
&\quad - 2w_1'(x)(c_1 w_2'(x)^2 - c_1 w_1''(x) + 2w_2'(x)w_2''(x))),\\
\beta_2(x) &= (3c_1 k_1 w_1'(x)^2 - 2k_1 w_1'(x)^3 + c_1 k_1 w_2'(x)^2 + w_1'(x)\\
&\quad \times (-c_1^2 k_1 + 2c_1 k_2 w_2'(x) - 2k_1 w_2'(x)^2 + 2k_1 w_1''(x))\\
&\quad + w_2(x)(-c_1^2 k_2 + 2k_1 w_2''(x)) - c_1(k_1 w^{''}(x)\\
&\quad + k_2 w_2''(x)))/(c_1(-2c_1 w_1'(x)^3 + w_1'(x)^4 + w_2(x)^4\\
&\quad + w_1'(x)^2(c_1^2 + 2w_2'(x)^2 - 2w_1''(x)) + w_1''(x)\\
&\quad + w_2'(x)^2(c_1^2 + 2w_1''(x)),
\end{aligned} \tag{17}$$

where c_1 and c_2 are real constants. Substituting Eqs. (10) and (17) into Eq. (7), we get the following expression of $A(z,x)$ as

$$A(z,x) = \frac{\varepsilon\, \mathrm{e}^{k_1 z + \mathrm{i}k_2 z + \theta_1 + \mathrm{i}\theta_2 + w_1(x) + \mathrm{i}w_2(x)}}{1 + c_2 \varepsilon^2\, \mathrm{e}^{c_1 x + 2k_1 z + 2\theta_1}}. \tag{18}$$

Then, combining Eq. (17) with Eqs. (4) and (6), we get the brief expression of $f(x)$ as

$$f(x) = c\, \mathrm{e}^{\int \frac{\alpha_1(x) + \mathrm{i}\alpha_2(x)}{2(\beta_1(x) + \beta_2(x))} \mathrm{d}x}. \tag{19}$$

Here c is a real constant similar with c_1 and c_2. In this part, the potential function is that $U(x) = V(x) + \mathrm{i}W(x)$. $V(x)$ and $W(x)$ are real functions which represent the real and imaginary parts, respectively. Through Eq. (4), we can get the foolowing expression of $V(x)$ and $W(x)$:

$$\begin{aligned}
V(x) &= \beta_2(x)\Big(\Gamma_2'(x) + 2\Gamma_1(x)\Gamma_2(x)\Big) \\
&\quad - \beta_1(x)\Big(\Gamma_1^2(x) + \Gamma_1'(x) - \Gamma_2^2(x)\Big), \\
W(x) &= -\beta_2(x)\Big(\Gamma_1^2(x) - \Gamma_2^2(x) + \Gamma_1'(x)\Big) \\
&\quad - \beta_1(x)\Big(\Gamma_2'(x) + 2\Gamma_1(x)\Gamma_2(x)\Big), \\
\Gamma_1(x) &= \frac{\alpha_1(x)\beta_1(x) + \alpha_2(x)\beta_2(x)}{2(\beta_1^2(x) + \beta_2^2(x))}, \\
\Gamma_2(x) &= \frac{\alpha_2(x)\beta_1(x) - \alpha_1(x)\beta_2(x)}{\beta_1^2(x) + \beta_2^2(x)}.
\end{aligned} \tag{20}$$

In order to obtain the expression of $u(z,x)$, we substitute Eqs. (18)–(19) into Eq. (2). Since its expression is very complex, here we only give its simplified form

$$\begin{aligned}
u(z,x) &= c\varepsilon\, \mathrm{e}^{\int \frac{\alpha_1(x) + \mathrm{i}\alpha_2(x)}{2(\beta_1(x) + \beta_2(x))} \mathrm{d}x} \\
&\quad \times \frac{\mathrm{e}^{k_1 z + \mathrm{i}k_2 z + \theta_1 + \mathrm{i}\theta_2 + w_1(x) + \mathrm{i}w_2(x)}}{1 + c_2 \varepsilon^2\, \mathrm{e}^{c_1 x + 2k_1 z + 2\theta_1}}.
\end{aligned} \tag{21}$$

Taking advantage of the parameters in Fig. 7, we can get diverse soliton structures of $u(z,x)$, and the corresponding potential function $U(x) = V(x) + \mathrm{i}W(x)$ meet PT-symmetric that the real part $V(x) = V(-x)$, and the imaginary component $W(x) = -W(x)$.

From Fig. 8 to Fig. 11, we can see that the structures of $u(z,x)$ vary with the potential function $U(x)$. In Figs. 8 and 9, the periodic wave structures were formed under the modulation of the potential function changing regularly. The periodic fields $V(x)$ can be regarded as the tight-binding model. Especially, in Fig. 8, the field center is a lattice defect that results in a more deeper trap. In Fig. 9, the structure of the periodic wave is more smooth. In Fig. 10, the soliton-like structure appears raised in the middle because of the system generating a gain which was decided by the trap of the bound potential. The PT gain distribution is balanced with the nonlinear and dispersive gain or loss exactly, which has not obvious influence on the soliton structure. In contrast to Fig. 10, the bound potential forms a barrier result in the system generating a loss in Fig. 11, so soliton-like structure appears sunken in the middle. From Figs. 10 and 11, we can design optical switches depending on the different amplitude of soliton-like structures which are formed by convex or concave in the middle of the structures.[62] In addition, the diffraction coefficient $\beta(x)$ and the nonlinearity $\gamma(x)$ can influence the amplitudes and pulse duration of the structures, and they can also change the propagation direction to a certain extent.

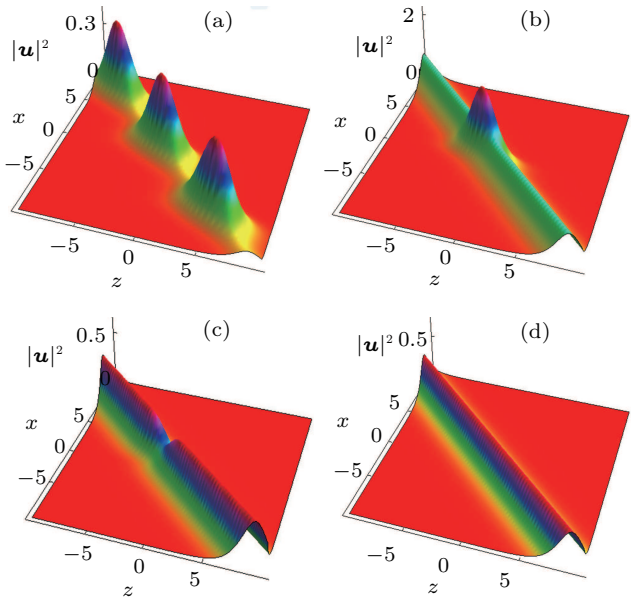


Fig. 7. (color online) Different soliton structures of $A(z,x)$ with the appropriate parameters as: $\varepsilon = 1$, $k_1 = 1$, $k_2 = 0.75$, $c_1 = 2$, $c_2 = 1$, and $\theta_i = 1$ $(i = 1,2)$. (a) Periodic wave structure $w_1(x) = x + \cos(x) - 1$ and $w_2(x) = 0.1\sin(x)$. (b) Soliton-like structure $w_1(x) = x + 0.8\,\mathrm{e}^{-x^2}$ and $w_2(x) = 0.1\sin(x)$. (c) Solition-like structure $w_1(x) = x - 0.5\,\mathrm{e}^{-x^2}$ and $w_2(x) = 0.1\sin(x)$. (d) Single soliton structure $w_1(x) = x$ and $w_2(x) = 0.1\sin(x)$.

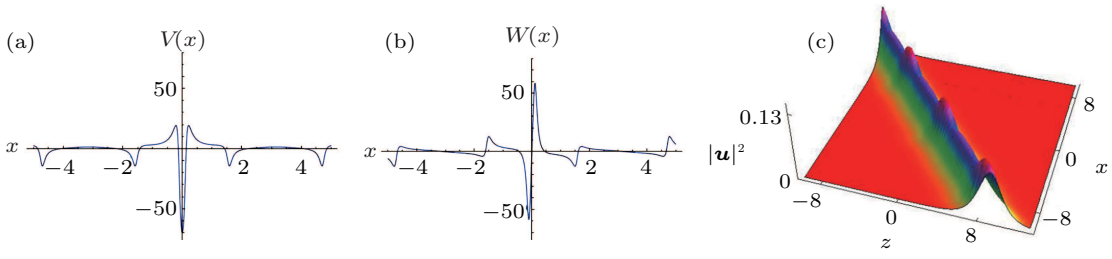


Fig. 8. (color online) The appropriate parameters are: $w_1(x) = x + \cos(x) - 1$, $w_2(x) = 0.1\sin(x)$, $\varepsilon = 1$, $k_1 = 1$, $k_2 = 0.75$, $c_1 = 2$, $c_2 = 1$, and $\theta_i = 1$ $(i = 1,2)$. (a) The real part of the corresponding potential function. (b) The imaginary component of the corresponding potential function. (c) Periodic wave structure of $u(z,x)$. Figure 9.

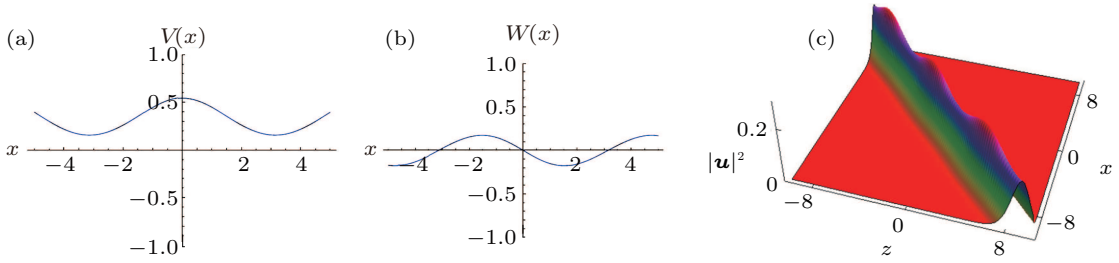


Fig. 9. (color online) The appropriate parameters are: $w_1(x) = x + 0.8\,\mathrm{e}^{-x^2}$, $w_2(x) = 0.1\sin$, $\varepsilon = 1$, $k_1 = 1$, $k_2 = 0.75$, $c_1 = 2$, $c_2 = 1$ and $\theta_i = 1$ $(i = 1,2)$. (a) The real part of the corresponding potential function. (b) The imaginary component of the corresponding potential function. (c) Soliton-like structure of $u(z,x)$.

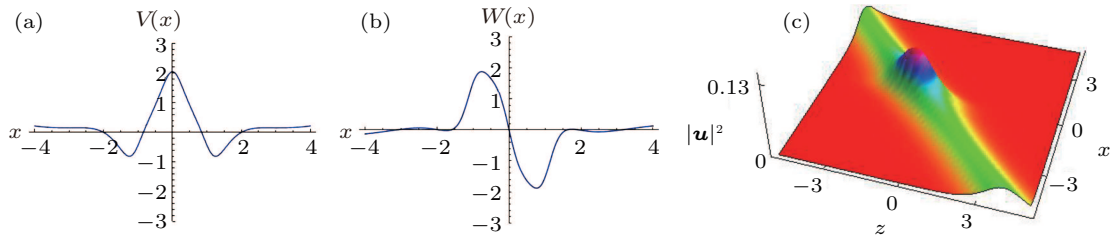


Fig. 10. (color online) The appropriate parameters are: $w_1(x) = x - 0.5\,\mathrm{e}^{-x^2}$, $w_2(x) = 0.1\sin(x)$, $\varepsilon = 1$, $k_1 = 1$, $k_2 = 0.75$, $c_1 = 2$, $c_2 = 1$, and $\theta_i = 1$ $(i = 1,2)$. (a) The real part of the corresponding potential function. (b) The imaginary component of the corresponding potential function. (c) Soliton-like structure of $u(z,x)$.

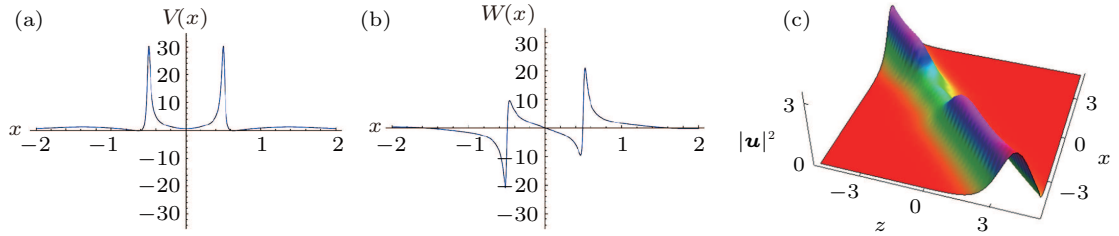


Fig. 11. (color online) The appropriate parameters are: $w_1(x) = x$, $w_2(x) = 0.1\sin(x)$, $\varepsilon = 1$, $k_1 = 1$, $k_2 = 0.75$, $c_1 = 2$, $c_2 = 1$, and $\theta_i = 1$ $(i = 1,2)$. (a) The real part of the corresponding potential function. (b) The imaginary component of the corresponding potential function. (c) Periodic wave structure of $u(z,x)$.

4. Conclusion

In this paper, we have studied the (1+1)-dimensional variable-coefficient CGL equation with a PT-symmetric potential, i.e., Eq. (1). We have divided it into two parts according to each parameter as complex or not, and got various soliton structures according to solutions (15) and (21) by the bilinear method. Here we have mainly considered the influence of PT-symmetry on the structure of $u(z,x)$, and derived various structures, such as single-soliton structure, periodic wave structure, soliton-like structure, and so on. The numerical simulation and stability against noises have been studied on the single-soliton structure. Furthermore, we can design all-optical switches depending on the different amplitudes of soliton-like structures which are formed by the convex or concave in the middle of the structures. In addition, the diffraction and nonlinearity can impact on the amplitudes and pulse duration of soliton structures. It may be meaningful to study the solutions of (2+1)-dimensional CGL equation with variable diffraction and nonlinearity coefficients in a PT-symmetric potential. The above analysis also plays a potential role in future experiments and applications of ultrafast optics.

References

[1] Bender C M and Boettcher S 1998 *Phys. Rev. Lett* **80** 5243
[2] Musslimani Z H 2008 *Phys. Rev. Lett.* **100** 030402
[3] Yan Z Y, Xiong B and Liu W M 2010 arXiv:1009.4023
[4] Yan Z Y 2013 *Philos. Trans. R. Soc. A* **371** 20120059
[5] Yan Z Y, Wen Z C and Konotop V V 2015 *Phys. Rev. A* **92** 023821
[6] Guo A, Salamo G J, Volatier-Ravat M, Aimez V, Siviloglou G A and Christodoulides D N 2009 *Phys. Rev. Lett.* **103** 093902
[7] Luo X, Huang J, Zhong H, Qin X, Xie Q, Kivshar Y S and Lee C 2013 *Phys. Rev. Lett.* **110** 243902
[8] Yan Z Y, Wen Z C and Hang C 2015 *Phys. Rev. E* **92** 022913
[9] Xu Y J and Dai C Q 2014 *Opt. Commun.* **318** 112
[10] Chen S and Dudley J 2009 *Phys. Rev. Lett* **102** 233903
[11] Chen L, Li R, Yang N, Chen D and Li L 2012 *Proc. Rom. Acad.* **13** 46
[12] Burlak G and Malomed B 2013 *Phys. Rev. E* **88** 062904
[13] Barashenkov I V 2014 *Phys. Rev. A* **90** 045802
[14] Yan Z Y, Chen Y and Wen Z C 2016 *Chaos* **26** 083109
[15] Chen Y and Yan Z Y 2017 *Phys. Rev. E* **95** 012205
[16] Wen Z C and Yan Z Y 2017 *Chaos* **27** 053105
[17] Yan Z Y and Chen Y 2017 *Chaos* **27** 073114
[18] Kartashov Y V, Malomed B A and Torner L 2011 *Rev. Mod. Phys.* **83** 247
[19] Dai C Q, Chen R P, Wang Y Y and Fan Y 2017 *Nonlinear Dyn.* **87** 1675
[20] Driben R and Malomed B A 2011 *Opt. Lett.* **36** 4323
[21] Chen Y and Yan Z Y 2016 *Sci. Rep.* **6** 23478
[22] Chen Y, Yan Z Y, Mihalache D and Malomed B A 2017 *Sci. Rep.* **7** 1257
[23] Yang J 2014 *Opt. Lett.* **39** 5547

[24] Lou C B, Song D H, Tang L Q, Chen X Y, Xu J J and Chen Z G 2008 *Physics* **37** 239

[25] Zhu X, Wang H, Zheng L X, Li H and He Y J 2011 *Opt. Lett.* **36** 2680

[26] Liu S, Ma C, Zhang Y and Lu K 2012 *Opt. Commun.* **285** 1934

[27] Abdullaev F K, Kartashov Y V, Konotop V V and Zezyulin D A 2011 *Phys. Rev. A* **83** 041805

[28] Zhou Z, Zhong H H, Zhu B, Xiao F X, Zhu K and Tan J T 2016 *Chin. Phys. Lett.* **33** 1

[29] Li C, Liu H and Dong L 2012 *Opt. Express* **20** 16823

[30] Zezyulin D A and Konotop V V 2012 *Phys. Rev. Lett.* **108** 213906

[31] Driben R and Malomed B A 2011 *EPL* **96** 51001

[32] Liu W J, Liu M L, Lei M, Fang S B and Wei Z Y 2018 *IEEE J. Sel. Top. Quant.* **24** 0901005

[33] Liu Y K and Li B 2017 *Chin. Phys. Lett.* **34** 010202

[34] Hua W, Liu X S and Liu S X 2016 *Chin. Phys. B* 25 050202

[35] Liu W J, Yu W T, Yang C Y, Liu M L, Zhang Y J and Lei M 2017 *Nonlinear Dyn.* **89** 2933

[36] Wang L, Zhang J H, Wang Z Q, Liu C, Li M, Qi F H and Guo R 2016 *Phys. Rev. E* **93** 012214

[37] Liu W J, Pang L H, Yan H, Ma G L, Lei M and Wei Z Y 2016 *EPL* **116** 64002

[38] Jia R X, Yan H L, Liu W J and Lei M 2014 *Chin. Phys. B* **23** 0100502

[39] Liu W J, Yang C Y, Liu M L, Yu W T, Zhang Y J, Lei M and Wei Z Y 2017 *EPL* **118** 34004

[40] Li Z D, Wu X, Li Q Y and He P B 2016 *Chin. Phys. B* **25** 010507

[41] Zheng Y, Tain J R, Dong Z K, Xu R Q, Li K X and Song Y R 2017 *Chin. Phys. B* **26** 074212

[42] Liu W J, Pang L H, Han H H, Bi K, Lei M and Wei Z Y 2017 *Nanoscale* **9** 5806

[43] Duan L N, Wen J, Fan W and Wang W 2017 *Chin. Phys. B* **26** 0104205

[44] Liu W J, Pang L H, Han H H, Liu M L, Lei M, Fang S B, Teng H and Wei Z Y 2017 *Opt. Express* **25** 2950

[45] Gao J H, Xie W M, Gao J Z, Yang H P and Ge Z C 2012 *Acta Phys. Sin.* **61** 130506

[46] Renninger W, Chong A and Wise F 2008 *Phys. Rev. A* **77** 023814

[47] Mihalache D, Mazilu D, Lederer F, Kartashov Y, Crasovan L C, Torner L and Malomed B 2006 *Phys. Rev. Lett.* **97** 073904

[48] Grelu P and Akhmediev N 2012 *Nat. Photon.* **6** 84

[49] He Y and Mihalache D 2013 *Phys. Rev. A* **87** 013812

[50] Feng L, Wong Z J, Ma R M, Wang Y and Zhang X 2014 *Science* **346** 972

[51] Hodaei H, Miri M A, Heinrich M, Christodoulides D N and Khajavikhan M 2014 *Science* **346** 975

[52] Liang Y and Alam M R 2013 *Phys. Rev. E* **88** 035201

[53] Gao X, Huang S, Song Y, Li S, Wei Y, Zhou J, Zheng X, Zhang H and Gu W 2014 *Opt. Lett.* **39** 2652

[54] Fu B, Gui L, Zhang W, Xiao X, Zhu H and Yang C 2013 *Opt. Commun.* **286** 304

[55] Lin Z, Ramezani H, Eichelkraut T, Kottos T, Cao H and Christodoulides D N 2011 *Phys. Rev. Lett.* **106** 213901

[56] Makris K G, Ganainy R E and Christodoulides D N 2008 *Phys. Rev. Lett.* **100** 103904

[57] He Y, Malomed B A and Mihalache D 2014 *Philos. Trans. R. Soc. A.* **372** 20140017

[58] He Y and Mihalache D 2013 *Phys. Rev. A* **87** 013812

[59] Yang J 2014 *Opt. Lett.* **39** 5547

[60] Liu W J, Huang L G, Huang P, Li Y Q and Lei M 2016 *Appl. Math. Lett.* **61** 80

[61] Yan Z Y 2010 *Phys. Lett. A* **374** 4838

[62] Izdebskaya Y, Rebling J, Desyatnikov A, Assanto G and Kivshar Y 2012 *Opt. Lett.* **37** 767

[63] Hossein H, Mohammad M A, Matthias H, Christodoulides D N and Mercedeh K 2014 *Science* **346** 975

[64] Yin C, He Y, Li H and Xie J 2012 *Opt. Express* **20** 19355

[65] Agrawal G 2009 *Nonlinear Fiber Optics*, 4th edn.